Vibro-acoustic optimisation of Wood Plastic Composite systems

Andrea Santoni[a,*], Paolo Bonfiglio[a], Francesco Mollica[a], Patrizio Fausti[a], Francesco Pompoli[a], Valentina Mazzanti[a]

[a]*Department of Engineering, University of Ferrara, via G. Saragat 1, 44122 Ferrara, Italy*

Abstract

"Wood Plastic Composite" or WPC is becoming increasingly popular in outdoor applications because of the advantage of a better durability in wet environments compared to natural wood. The possibility of using WPC as a sound barrier, or as façade cladding, is investigated in this paper. The sound transmission loss (TL) of an orthotropic WPC panel, obtained by coupling together several boards, is computed by means of the transfer matrix method. The plate is modelled as a thin orthotropic layer, described by frequency dependent elastic properties. A numerical procedure, based on a finite element simulation, is proposed in order to determine the stiffness properties along the principle direction of the panel. The reliability of this approach is verified by comparing the numerical results with the experimental stiffness measured on a WPC beam. The orthotropic behaviour is approximated by an elliptic interpolation of the flexural stiffness along the two principle directions, based on a simplified assumption which considers the in-plane shear modulus proportional to the orthotropic elastic moduli. The model based within the transfer matrix method framework is validated with the experimental transmission loss measured on a WPC panel in a reverberant room. Finally, the possibility of increasing the acoustic performance of WPC structures by optimising their cross-section is investigated.

Keywords: Wood Plastic Composite, vibro-acoustic optimisation, FEM analysis

1. Introduction

Besides widely accepted benefits of environmental friendliness, natural-fibre-filled polymers are interesting materials due to their convenient balance of mechanical properties and cost. Natural fibres, in fact, are relatively cheap, as they originate from local agricultural or industrial waste. Although traditional reinforcement, like glass fibres, impart higher stiffness and strength, the mechanical properties of natural-fibre-filled plastics are usually adequate. Among natural fibres, wood flour is one of the most widely used filler, mainly because of its wider availability. The resulting material is often termed "Wood Plastic Composite" or WPC and is becoming increasingly popular as a wood substitute. The WPC market share has expanded in the last twenty years by an average annual growth around 3.0% [1, 2] and the trend is still increasing. The main advantage with respect to natural wood is outdoor durability, also in a wet environment, which allows applications like external flooring, decking, fences, and near-water structures such

*Corresponding author
Email address: andrea.santoni@unife.it (Andrea Santoni)

as piers. WPC boards can be processed with standard woodworking procedures, e.g. sawing and drilling, but at the same time they can be extruded like a standard plastics profile, thereby allowing engineering-optimized sections that are usually not obtainable with natural wood. The main research activities concerning WPC that are available in the scientific literature aim at improving the mechanical properties of the material, i.e. strength and stiffness, usually by acting on the WPC composition [3]. The main factors that are considered are the presence and quantity of additives, e.g. the coupling agents, and the amount, quality and geometrical properties of the wood fibres in the formulation. It is normally found that the optimum properties are obtained using a wood fibre filling level of about 50 wt.%, the fibres possessing an aspect ratio of 10 or higher and using an amount of coupling agent around 4 wt.% [4, 5]. Mechanical properties may also be improved by using polypropylene as the matrix [6, 7], which on the other hand has the drawback of a more difficult processing and characterization [8].

In this article we explore the possibility of using WPC boards as a sound barrier or a façade cladding system, which are relatively new fields of application. To the best of our knowledge, there are very few studies that are concerned with the acoustic performance of such structures. The acoustic performance of wood-polymer composites has been previously investigated, however, research so far has been mainly focused on sound absorption of composite foams [9] and different sustainable composites [10, 11], rather then on sound insulation provided by this kind of materials. Zhao et al. [12] investigated the normal incidence sound insulation of wood-rubber composite panels by using a four-microphone measurement technique. In order to simulate the sound transmission loss (TL) of an orthotropic WPC panel, which is constructed by binding together several boards, the transfer matrix method (TMM) is used [13], although to implement this method it is necessary to know the stiffness characteristics of the investigated element. The material dynamic elastic modulus is firstly derived by means of a standard procedure. The apparent frequency-dependent flexural stiffness of a WPC extruded board is then determined numerically and verified with experimental data. By means of frequency-dependent stiffness properties the dynamic response of complex structures, such as sandwich beams or WPC boards, can be approximated with good accuracy using low-order theories [14]. Furthermore, in order to describe the orthotropic behaviour of the WPC board, the stiffness characteristics should be determined along both principle directions [15]. To this purpose, a numerical approach based on Finite Element (FE) simulations, is presented and validated with numerical results.

In the present paper a noise barrier has been constructed by coupling together several WPC boards. The sound insulation provided by this panel has been tested in a reverberation room coupled with a semi-anechoic chamber. This method allows a much more accurate measurement with respect to the impedance tube method, as it considers a diffuse incident sound field, and more realistic boundary conditions. The experimental transmission loss is used to validate the numerical model based on the TMM framework. Finally, thanks to the possibility of easily varying the profile cross-section by changing the extrusion die, an optimized shape of the cross section has also been simulated by numerical computation using the methods described in section 4.

2. Material and methods

The material used in this investigation was a commercial WPC board manufactured by Iperwood srl (Ferrara, Italy). This material is a high density polyethylene (HDPE) filled with 50 wt.% of wood fibres from pine sawdust.

Published article available online: https://doi.org/10.1016/j.conbuildmat.2018.04.155

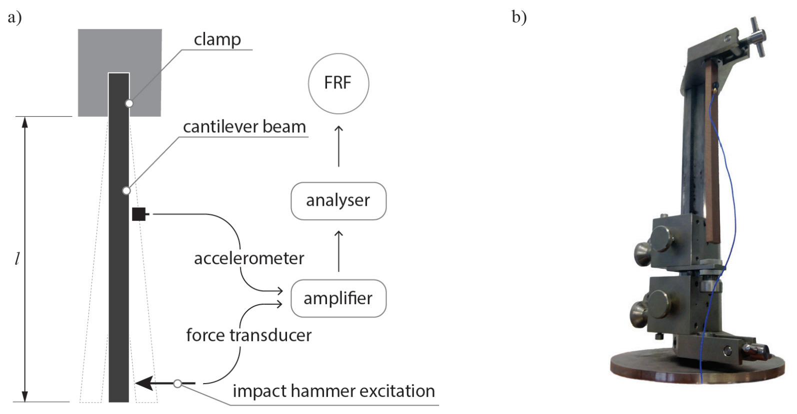

Figure 1: Oberst beam method: a) Diagram of the experimental setup; b) Picture of the measurements performed in UNIFE laboratory on a homogeneous WPC bar.

In order to investigate the vibro-acoustic behaviour of WPC elements it is necessary to dynamically characterise both the material's properties and the dynamic response of the entire system. Acoustically excited structures exhibit very small deflections. Thus, according to the the small strain assumption, WPC can be assumed as a linear viscoelastic material, characterised by a complex elastic modulus taking into account the energy dissipation due to viscous damping. Moreover, the dynamic response of elements with complex structural geometries can be approximated by means of low-order theories, using frequency dependent elastic properties.

2.1. Material characterisation

The "Oberst beam" is a classical method to dynamically characterise the elastic and damping properties of viscoelastic materials. The methodology, described in the ASTM E756 standard [16], is based on the analysis of the Frequency Response Function (FRF) measured on a clamped-free homogeneous bar. The element should be excited by an electromagnetic transducer, in order not to interfere with its response. Unfortunately, WPC is not a ferromagnetic material and it was necessary to excite the bar mechanically in a different way. An alternative setup to apply Oberst's technique was proposed by Wojtowicki et al. [17]. It was compared to other experimental techniques to determine the elastic and damping properties in Ref. [18], showing that, with contacting piezoelectric transducers, it is necessary to perform a large number of measurements in order to experimental dispersion and obtain more accurate results, especially at low frequencies where the resulting loss factor is usually highly fluctuating and characterised by significant variability. A homogeneous WPC bar was excited by using an impact hammer equipped with a force transducer, as shown in in Figure 1. It is possible to determine the elastic modulus of the homogeneous elastic material from the resonance frequencies of the bar, evaluated from the measured FRF, as [16]:

$$E = \frac{12\rho l^4 f_n^2}{h^2 C_n^2}, \tag{1}$$

where ρ is the material density, l is the bar's length and h its thickness, f_n is the resonant frequency of mode n, while C_n represents a coefficient of the clamped-free beam associated with mode n, given in the E756 ASTM standard [16] and reported in Table 1. In order to verify the reliability of the results, the dynamic elastic modulus was compared with the static Young's modulus.

Static Young's modulus was determined with the three-points bending method according to the ASTM D790 standard, using an INSTRON 4467 dynamometer equipped with a 500 N full scale load cell. Four specimens in the form of 23 mm × 4.5 mm rectangular cross section bars cut along the longitudinal extrusion direction were loaded in the central section of a 80mm span at room temperature. Since the Young's modulus had to be compared with the stiffness coming from measurements performed at high loading frequencies, the highest allowable cross-head speed was used, i.e. 200 mm/min. Following the three-points bending method, the stress σ could be obtained by

$$\sigma = \frac{3}{2}\frac{FL}{bh^2}, \tag{2}$$

while the strain ε can be obtained by

$$\varepsilon = \frac{6\delta h}{L^2} \tag{3}$$

In the above formulae, L is the span, F is the force as measured by the load cell, δ is the cross head displacement that is supposed to be equal to the specimen displacement and h and b are the specimen thickness and width respectively. Young's modulus E can then be obtained as usual

$$E = \frac{\sigma}{\varepsilon} \tag{4}$$

2.2. Dynamic response of a sandwich beam

WPC beams are normally obtained by extrusion, therefore lightweight structures can be easily realised using alveolar or cellular cross sections e.g. Figure 2. These can be seen as two horizontal laminae that are transversely connected through regularly spaced solid elements of the same material.

In vibro-acoustic analysis, WPC beams, due to their inner structure, can be treated as sandwich elements, particular structures in which two thin laminae are separated by an inner lightweight core. The dynamic response of a sandwich beam can be determined, according to a well-established model proposed by Nilsson [19], by analysing laminates using the classical Euler-Bernoulli theory, while the inner core is described by general field equations. Both the external laminae and the core are assumed to be isotropic elements. The sandwich beam is thus characterised by an apparent frequency-dependent bending stiffness D that takes into account shear, rotation and longitudinal deflection of the core, other than pure bending of the outer layers. For mode n of a free-free sandwich beam the apparent global bending stiffness can be approximated as [19, 20]:

$$D_n = \frac{4Ml^3 f_n^2}{\pi^2 b\,(n+0.5)^4} \tag{5}$$

where M is the beam's total mass, l its length, b its width, and f_n the resonant frequency associated with mode n. This simplified approach provides a good approximation of the structure's dynamic response if compared with higher order theories, as discussed in Ref. [21]. This approach was applied by modelling a free-free WPC beam with a finite element (FE) code, computing the resonance frequencies in order to determine its bending stiffness according to Eq. (5). The model was validated by comparing the numerical results with the experimental resonance frequencies obtained from the dynamic response measured on a WPC beam 1.43 m long, 0.145 m wide and 0.025 m thick. The free-free boundary conditions were simulated by suspending the structure

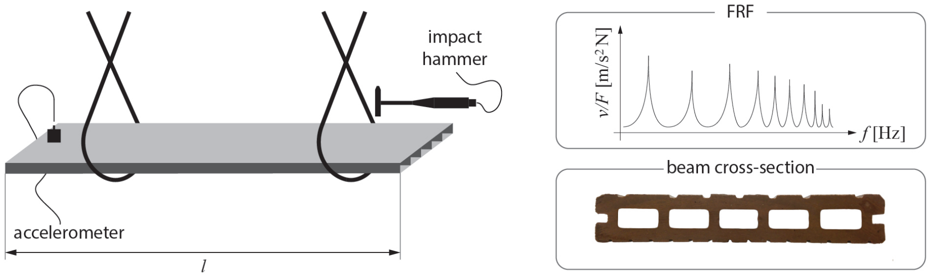

Figure 2: Digram of the experimental setup to measure the FRF of a freely suspended beam and a picture of the WPC beam cross section.

with elastic bands as shown in the diagram of Figure 2. The motion due to an impact hammer excitation on one end of the beam was measured with a small accelerometer placed on the opposite end. From the resonance frequencies, obtained from the measured FRF, it was also possible to determine the structural damping by means of the half-power bandwidth method [22].

2.3. Stiffness properties of an orthotropic structure

Extruded WPC beams are assembled and joined together in order to make a plate-like structure, similar to those used in many applications. Due to the geometric configuration of their substructure, these panels present a different stiffness along the two principal directions, which are aligned with the plate's edges. The stiffness properties of such an orthotropic plate were investigated numerically. In order to develop a computationally efficient procedure, one can derive the orthotropic properties by analysing two perpendicular beams, cut along the plate's principal directions, rather that modelling the entire panel, as shown in Figure 3. The apparent bending stiffness along the x-direction $D_{x,n}$ can be determined for any resonance frequency computed from an FEM model of the extruded WPC beam, as described in section 2.2. In an analogous way, it is possible to investigate the resonant response of an orthogonal bar, modelled in an FE code as a certain number of beam sections, coupled together by a continuity condition. From the resonance frequencies of the beam's FRF, the apparent bending stiffness $D_{y,n}$ along the principal y-direction can be computed according to Eq. (5). The sandwich element can be treated as an equivalent homogeneous orthotropic structure, characterised by a frequency-dependent bending stiffness associated to the principal directions: D_x and D_y. This allows to describe the structural dynamic behaviour by means of a simpler theory. The dynamic elastic, or stiffness, properties approach the static value when the frequency tends to zero, while as the frequency increases it decays asymptotically down to a constant value. In order to obtain accurate vibro-acoustic simulated results by using an apparent frequency dependent bending stiffness, it is necessary to known this parameter within the entire frequency range: from the lower frequencies up to the higher investigated ones. However, due to the computational complexity, combined with FEM mesh size requirements, it is often possible only to evaluate the resonances within a limited frequency band. Fortunately the bending stiffness of sandwich-like structures can be fitted within the entire investigated range according to the relationship [14]:

$$\frac{A}{f} D_i^{3/2}(f) - \frac{B}{f} D_i^{1/2}(f) + D_i(f) - C = 0 \tag{6}$$

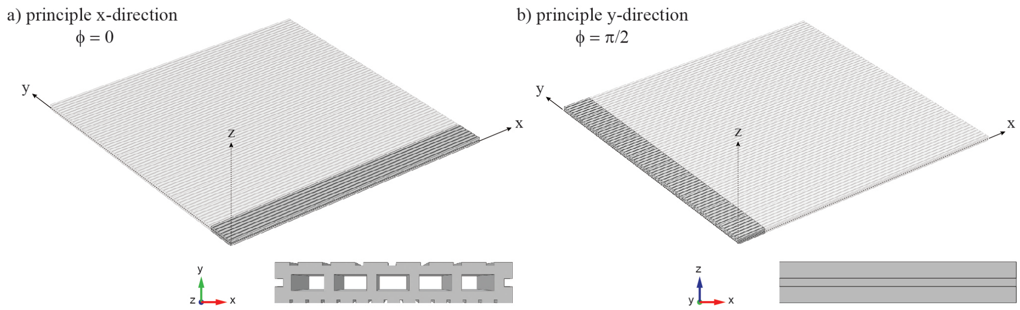

Figure 3: FEM model of the two principal directions of a WPC orthotropic plate: a) x-direction (extruded beam); b) y-direction sections beam

where the subscript i indicates the plate's principal direction: $i = x, y$.

The constants A, B, and C can be determined from a mean square minimisation of Eq. (6) evaluated at the beam's resonance frequencies $f_{n,i}$. It is well known that at very low frequencies the dynamic response of an sandwich beam is governed by its static bending stiffness D_s, computed from the elastic moduli of the core and of the laminae E_c, E_l and the associated thicknesses h_c and h_l respectively: [14]:

$$D_s = \frac{E_c h_c^3}{12} + E_l \left(\frac{h_c^2 h_l}{2} + h_c h_l^2 + \frac{2h_l^3}{3} \right) \tag{7}$$

however, as the frequency increases and tends to ∞, the bending stiffness approaches asymptotically a constant value represented by the bending stiffness per unit of length of the external laminae D_l of a symmetric sandwich element.

$$D_l = \frac{E_l h_l^3}{12} \tag{8}$$

Therefore, it is possible to increase the accuracy of the minimisation algorithm by reducing the number of variables, i.e. A, B and defining the constant C, which represents the stiffness at high frequencies, as:

$$C = 2D_l \tag{9}$$

For the studied WPC structure D_l has been computed as the bending stiffness of a homogeneous thin beam with thickness $h_l = 0.0075$ m and $E_l = \overline{E}_{Ob.}$, which is the average WPC elastic modulus experimentally determined by using the Oberst method, as described in section 2.1 and given in Table 1. This approximate method only applies to sandwich structures. Alternatively, the apparent stiffness associated with the principal directions of the WPC beams can be evaluated, within a wide frequency range, from the structural wavenumbers obtained by using the classical spatial Fourier transform SFFT, as described and compared with other methods by Van Damme and Zemp [23] and by Roozen et al. [24]. While it is difficult to evaluate flexural modes implementing resonant techniques up to high frequencies, both numerically and experimentally, it is straightforward to determine the vibrational fields in terms of acceleration $a(t, x)$, velocity $v(t, x)$ or transverse displacement $w(t, x)$. For any investigated frequency, within the range

100 Hz ÷ 5000 Hz, the complex vibration velocity distribution has been evaluated, on the same FEM models implemented for the eigenfrequency analysis previously described, along a line of points parallel to the beam's axis, spaced 1 cm from one another. The complex vibration velocity $v(x, y)$ can be transformed from the spatial domain to the wavenumber domain by means of a spatial Fourier transform $\mathcal{F}$:

$$\begin{cases} v(k_x, \omega) = \mathcal{F}v(x, \omega) \\ v\left(k_y, \omega\right) = \mathcal{F}v(y, \omega) \end{cases} \tag{10}$$

For each frequency, the real part of the flexural wavenumber is easily determined by maximising the velocity $v(k_i, \omega)$. Under the thin plate assumption, the bending stiffness associated to each principal direction can be determined from Kirchhoff's dispersion relation:

$$D_i = \frac{\omega^2 \mu}{k_i^4} \tag{11}$$

where μ is the effective plate's mass per unit of surface.

Under a simplifying assumption that computes the in-plane shear modulus G_{xy} as a function of the elastic moduli E_x E_y [25], the orthotropic plate's bending stiffness can be approximated, from an elliptic interpolation of the structural wavenumber associated with the principal directions [15, 26], as:

$$D(\phi) = \left[D_x^{1/2} \cos^2 \phi + D_y^{1/2} \sin^2 \phi\right]^2 \tag{12}$$

where ϕ represent the propagation angle of the structural wave, measured to the x-axis. The energy dissipation can be taken into account by using a complex bending stiffness given by:

$$\overline{D} = D(1 - \mathrm{i}\eta_{tot}) \tag{13}$$

The plate's total loss factor η_{tot} can be computed as the sum of the structural viscous damping η_0 and the radiation damping η_{rad}, considering the same fluid medium on both sides of the plate, as [27]:

$$\eta_{tot} = \eta_0 + 2\eta_{rad} \tag{14}$$

The structural loss factor was determined from the FRF measured on the extruded beam, as already mentioned in the previous section, while the radiation damping can be computed as:

$$\eta_{rad} = \frac{\rho_0 c_0 \sigma}{\omega \rho h} \tag{15}$$

where ρ_0 is the air density, c_0 is the speed of sound, and σ represents the WPC plate's radiation efficiency. It was approximated considering only the resonant response of the orthotropic plate [28, 29].

2.4. Sound transmission loss of a WPC plate

A numerical model to evaluate the sound transmission loss (TL) provided by a WPC orthotropic plate is described in this section. In the literature many different approaches to predict the sound transmission loss of an orthotropic plate can be found. Guyader and Lesueur investigated sound transmission through multilayer orthotropic panels, considering both an oblique incident plane wave [30], and a diffuse field excitation [30, 31]. An analytic model, developed by Nilsson to investigate sound transmission through a sandwich panel, was applied by Piana

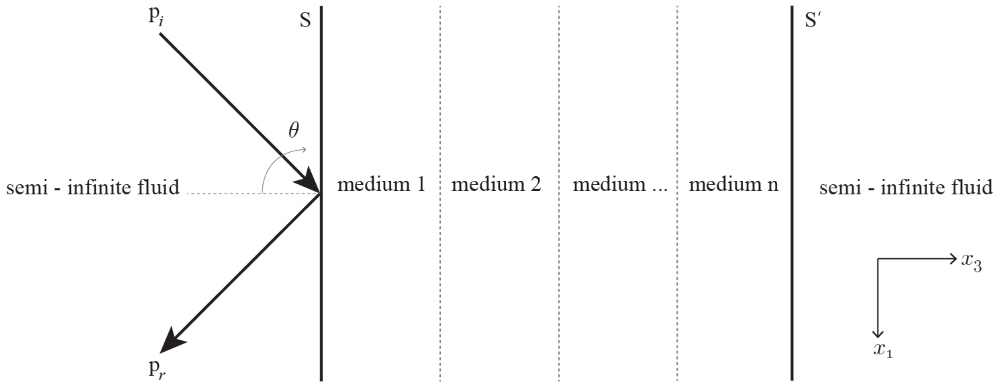

Figure 4: TMM diagram: acoustic wave impinging on a stratified structure with an incidence angle θ. The multilayer element is surrounded by a semi-infinite fluid on both sides.

et al. to orthotropic gypsum panels [26]. Recently, sound insulation of plywood panels, characterised by soft orthotropy, has been studied by Wareing, Davy and Pearse [32], taking into account the finite dimension of the plate, by means of the geometrical radiation impedance. Lin, Wang, and Kuo [33] developed a two-dimensional model within the transfer matrix framework, assuming in-plane isotropy, i.e. with the stiffness properties along the z-direction, which differ from the properties in the $x-y$ plane. The model was then extended by Kuo et al. [34], for the three-dimensional case, describing an orthotropic elastic solid characterised by the stress and strain relationship defined by nine independent constants. The model presented here was derived within the transfer matrix framework for a thin orthotropic layer, by drawing inspiration from the work presented by Atalla [35]. The transfer matrix method (TMM) is a powerful tool, with wide-range applicability [36, 37, 38], to model wave propagation through laterally infinite media of different nature, considering a two-dimensional problem of a plane acoustic wave impinging at an angle θ on the surface S of the element, as shown in Figure 4. The general TMM formalism can be expressed as:

$$\begin{Bmatrix} p_S \\ v_S \end{Bmatrix} = \begin{bmatrix} 1 & -Z(\omega, \phi) \\ 0 & 1 \end{bmatrix} \begin{Bmatrix} p_{S'} \\ v_{S'} \end{Bmatrix} \tag{16}$$

The acoustic pressure p_S and the particle velocity v_S completely define the acoustic field on the surface S. Analogously, $p_{S'}$ and $v_{S'}$ describe the acoustic field on the surface S'. Wave propagation through the WPC structure is described in terms of the plate's mechanical impedance $Z(\omega, \phi)$, given by:

$$Z(\omega, \phi) = \mathrm{i}\omega\rho h \left(1 - \frac{D(\phi)\, k_t^4}{\omega^2 \rho h}\right), \tag{17}$$

where h is the thickness of the plate, ρ its density, D the orthotropic bending stiffness, given in equations (12) and (13), and k_t is the trace wavenumber, defined as a function of the acoustic wavenumber k_0 as: $k_t = k_0 \sin\theta$.

At a given angular frequency ω, the transmission coefficient τ_∞, dependent on the propagation direction ϕ, can be determined by coupling the matrix given in Eq. (16) with a plane sound

Table 1: Dynamic elastic properties of a WPC bar determined for different resonant frequencies f_n using Oberst beam methods.

mode	f_n [Hz]	$E_{Ob.}$ [GPa]	C_n	$\overline{E}_{Ob.}$ [GPa]	ρ [kg/m^3]	l [m]	h [m]
1	119	5.43	0.55959	5.4	1316	0.142	0.0073
2	741	5.37	3.5069				
3	2085	5.43	9.8194				
4	4084	5.43	19.242				

wave impinging at a certain angle θ, and to a semi-infinite fluid on the receiving side, as accurately described in Chapter 11 of Ref. [39]. Assuming each medium to be infinitely extended on the sides, The TMM neglects both the modal resonances and diffraction effect caused by the finite dimension of real structures. Therefore in the low frequency range, the results may not accurately approximate the effective transmission loss. In order to increase the accuracy of the model, a geometrical radiation efficiency σ_{finite} was introduced to consider the diffraction due to the finite size of the element; which, however, also does not take into account modal resonances. The finite size transmission coefficient is thus given by:

$$\tau_f(\theta) = \tau_\infty(\omega, \theta, \phi)\,\sigma_{finite}(\omega, \theta, \phi)\cos\theta. \tag{18}$$

The non-resonant radiation efficiency σ_{finite} can be computed following either the approach proposed by Villot et al. [40] using the spatial windowing technique, or a more general one, proposed by Rhazi and Atalla [41], based on Rayleigh's integral formulation. Since both these methods are computationally expensive, several authors have proposed simplified approaches providing a faster algorithm, see for example [42, 43], although those are not suitable for orthotropic structures. Assuming a random incidence diffuse field excitation, the WPC plate's sound transmission loss is determined for each angular frequency ω as:

$$TL = -10\log\frac{\displaystyle\int_0^{2\pi}\int_0^{\pi/2}\tau_f(\omega, \theta, \phi)\sin\theta\cos\theta\,d\theta d\phi}{\displaystyle\int_0^{2\pi}\int_0^{\pi/2}\sin\theta\cos\theta\,d\theta d\phi} \tag{19}$$

3. Results and discussions

Applying Oberst's beam method, the dynamic elastic properties of a WPC homogeneous bar were determined from the first four resonances of the measured FRF, obtaining an almost constant value of Young's modulus, as reported in Table 1. The dynamic elastic modulus was also compared with the static Young's modulus measured with the three-points bending method. The four specimens that were tested had the following Young's moduli: 4.04, 4.09, 3.94 and 4.17 GPa, which lead to an average static Young's modulus of 4.06 GPa, as reported in Table 2, with a standard deviation of 0.08 GPa. These results are overall consistent with the measurement of the dynamic elastic properties using Oberst's method. Even though, probably due to the higher strain rate which characterises Oberst method, the dynamic elastic modulus is slightly higher than the static value obtain from the three-points bending method. In order to analyse the vibro-acoustic

Table 2: Static elastic properties of a WPC bar determined on four samples by means of the three-points bending method.

sample	$E_{3-p.}$ [GPa]	$\overline{E}_{3-p.}$ [GPa]	ρ [kg/m^3]	l [m]	h [m]
1	4.04	4.06	1316	0.142	0.0073
2	4.09				
3	3.94				
4	4.17				

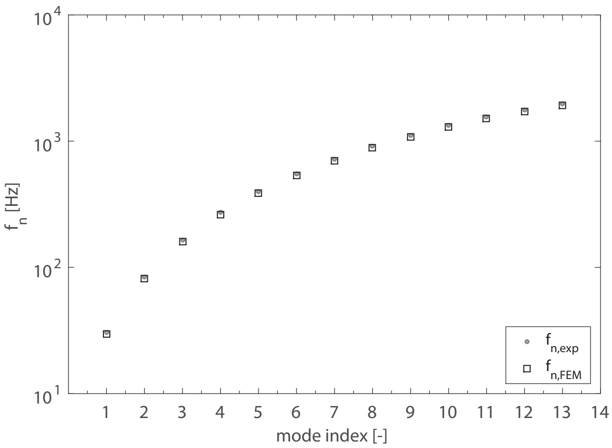

Figure 5: Comparison between the numerical and experimental resonance frequencies associated with bending motion of a WPC boards.

behaviour of WPC elements used in practical applications, it is necessary to take into account their geometry. The boards, obtained by extrusion, usually present a periodic cross section, alternating at regular steps a double-leaf system to a solid element. Adopting a well-established homogenisation technique commonly applied to sandwich elements, the WPC beam was analysed by means of a low-order theory compensated by frequency-dependent elastic properties. A free-free WPC beam was modelled with an FE code computing the resonance frequencies in order to determine its bending stiffness. The model was validated with experimental data measured on a freely suspended beam. It was possible to measure the first 13 resonances, associated with bending motion. The experimental and numerical resonance frequencies, compared in Figure 5, show a remarkable agreement. Due to the geometry of its substructure, the WPC plate, consisting of laterally connected beams, exhibits an orthotropic behaviour that was characterised by means of numerical investigation of the bending stiffness along the two principal directions.

As shown in Figure 6, a very good agreement was found between the wavenumbers obtained by using Kirchhoff's dispersion relation from the bending stiffness, computed from the resonant frequencies of flexural modes then extended in a wider frequency range using Eq. (6), and the wavenumbers determined by means of the more general approach based on spatial Fourier's transform SFTT. Only a small deviation is found at high frequencies, especially for the wavenumbers along the y-direction. In the same Figure the acoustic wavenumber k_0 is also shown, in order

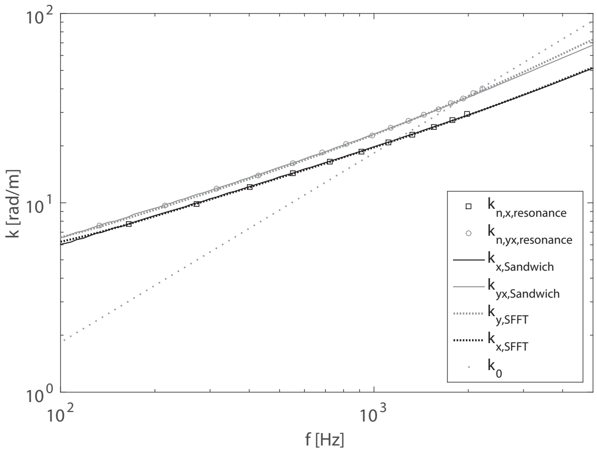

Figure 6: Bending wavenumbers determined along the two principal directions of a WPC plate by means of FEM simulations: comparison between the values computed at the resonances $k_{n,i,resonance}$, the values extend in frequency $k_{n,i,Sandwich}$, and the dispersion curves obtained from SFFT approach $k_{n,i,SFFT}$. The acoustic k_0 wavenumber is also reported.

to highlight the two characteristic coincidences of the orthotropic panel. The x-direction $\phi = 0$, associated with the extruded beam is the stiffest one within the entire frequency range. The coincidence associated with a flexural wave propagating along this direction falls around 1100 Hz, while the coincidence associated with the orthogonal y-direction $\phi = \pi/2$, which also represents the critical condition of the panel,falls around 1800 Hz.

In order to validate the sound transmission model, the transmission loss of a WPC plate was experimentally determined. Experimental tests were carried out into the sound transmission laboratory of the University of Ferrara. A rectangular panel, with dimensions $L_x = 1.50$ m, $L_y = 1.25$ m and $h = 0.025$ m, was mounted on a frame between a reverberant room, with a volume of 250.7 m^3, and a semi-anechoic chamber, as shown in Figure 7. In the reverberant room different sound sources were driven by a stationary white noise, and the average sound pressure level L_p was measured using six microphones placed in different positions. The receiving room had highly absorbing lateral walls and ceiling and a reflective floor. The average sound intensity L_i was measured inside this room at a distance of approximately 15 cm from the panel, by a manual scanning procedure using a B&K 3547 sound intensity probe. According to ISO 15186-1:2003 Standard [44] the plate's sound transmission loss TL_{exp} was calculated as:

$$TL_{exp} = L_p - L_i - 6 \tag{20}$$

The TL obtained from the FTMM model is compared with the experimental results in Figure 8. Two predicted curves of TL, computed with the FTMM, are shown: one was obtained using the bending stiffness determined from the resonant frequencies and the analytical formulation for sandwich elements given in Eq. (6), while for the other one the bending stiffness was determined, according to the dispersion relation given in Eq. (11), from the wavenumbers evaluated by means of the SFFT approach. Both numerical curves of TL are in good agreement with the experimental data. The finite-size correction provides a good approximation of the trend in the low frequencies, while in the mid-high range the simulated TL matches almost perfectly the

Published article available online: https://doi.org/10.1016/j.conbuildmat.2018.04.155

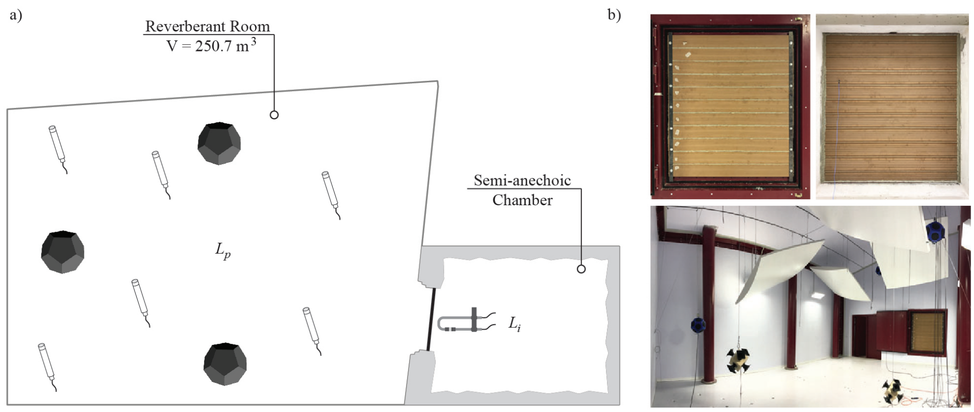

Figure 7: a) Diagram of the laboratory test facility for TL measurements; b) pictures of the experimental setup for TL measurement on the WPS plate

experimental data. The first coincidence associated with the stiffest direction and the critical condition of the WPC plate are close, falling in neighbouring bands and overlapping their associated dips in a wide region from 1250 Hz to 2000 Hz.

While below the critical condition, the two predicted TL are identical, since this is a mass-controlled region, at the highest frequencies a slight difference is found. The TL associated with the bending stiffness derived by using the SFFT seems to underestimates the experimental results, although the maximum deviation is lower than 2 dB. It should be mentioned that the SFFT approach is easily applicable to any kind of structure up to high frequencies, both numerically and experimentally, while it is difficult to evaluate the resonant frequencies associated with flexural modes in a wide frequency range. Moreover, the analytical formulation given in Eq. (6) is only valid for sandwich elements.

Concerning the material, wood flour as well as other natural fibers, have a rather low degradation temperature, i.e. around 200°C. This sets an upper bound on the processing temperature and eventually limits the choice of the thermoplastic matrix to be used, in the sense that the polymer must be molten and sufficiently fluid well below 200°C. Other than polyethylene only a few thermoplastics can be used as matrices of natural fiber filled materials, namely polypropylene (PP), polystyrene (PS) and polyvinylchloride (PVC). Polypropylene melts around 165°C limiting the processing temperature window to a very narrow range. Polystyrene is a very brittle thermoplastic that is not appropriate in structural applications. PVC, on the other hand, is often used as a matrix for WPCs, but it is usually much stiffer than polyethylene, its glass transition temperature being of the order of 70°C – 80°C. As a result, wood filled PVC would definitely be more rigid and this would negatively affect its acoustic properties. Quite recently also polyurethane has been used as WPC matrix [9], but in this case the manufacturing technique differs significantly from the extrusion that is used to produce the WPC decking profiles characterized in this work.

Typically, HDPE has relatively low mechanical properties, but adding a wood flour content of 50 wt.% allows to obtain stiffness and strength that are sufficient for weakly structural applications. Interestingly, the increase in mechanical properties correspond to an increase in dissipation. From standard formulae of dynamic mechanical analysis, the energy density W which is

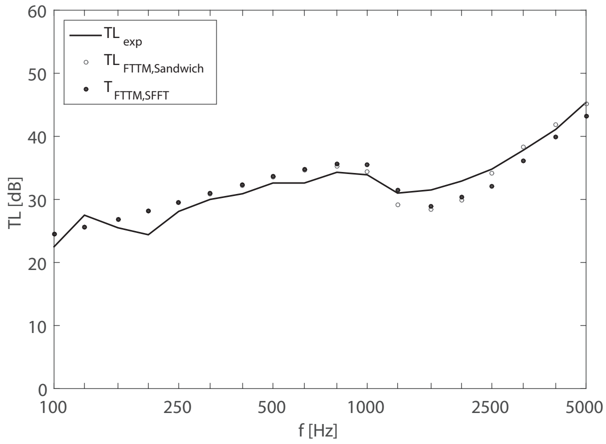

Figure 8: Comparison between experimental transmission loss of the WPC orthotropic plate TL_{exp} and FTMM results: $TL_{FTTM,Sandwich}$ represents the TL computed by using the apparent bending stiffness obtained from the resonance frequencies; $TL_{FTTM,SFFT}$ is the TL computed by using the apparent bending stiffness obtained from SFFT approach.

dissipated in a single sinusoidal cycle is:

$$W = \pi\varepsilon_0^2 E'' \tag{21}$$

where ε_0 is the strain amplitude and E″ is the loss modulus of the material. It can be shown [7] that E″ in wood flour filled polyolefins increases with wood content. Specifically, for the measurements reported in [7], the numerical value for the neat matrix is 44.8 MPa, for the 30 wt.% is 49.0 MPa and for the 50 wt.% is 54 MPa. For these reasons, adding wood filler to polyolefin does have a vibration damping effect.

4. System optimisation

Several factors, such as the kind of foaming used in the production process of the WPC, may influence the material's density and its elastic properties. Figure 9 shows a comparison between the different TL, computed by means of the FTMM, of WPC plates made out of boards with the same geometry by varying the material's density: $\rho_1 = 1316\text{kg/m}^3$, $\rho_2 = 1100\text{kg/m}^3$ and $\rho_3 = 900\text{kg/m}^3$.

A parametric analysis on the extruded beam has been performed by varying three geometric parameters, as shown in Figure 10, obtaining 28 configurations with different stiffness and different mass. The details of each investigated beam are given in Table 3.

The 28 investigated configurations provide different curves of TL. In order to understand how the geometric characteristics of the element influence its acoustic performance, it may be useful to show those configurations which represent limit cases, either in terms of mass for unit of surface or stiffness, rather than the results of all 28 configurations. In Figure 11, the TLs computed for 9 of the 28 parametric configurations are shown. It is clear that below the critical condition the surface mass governs the acoustic performance. In this frequency range the highest sound insulation is provided by the homogeneous plate, configuration 28, which has a surface

Published article available online: https://doi.org/10.1016/j.conbuildmat.2018.04.155

Table 3: Parametric configurations of the extruded WPC beam investigated.

Config.	a_1[mm]	a_2[mm]	a_3[mm]	h[mm]	$\mu\left[\frac{\text{kg}}{\text{m}^2}\right]$	R_w [dB]
1	5.0	5.0	17	20	21.6	34
2	5.0	5.0	20	20	20.9	34
3	5.0	5.0	23	20	20.2	33
4	5.0	10	17	20	17.7	32
5	5.0	10	20	20	16.3	31
6	5.0	10	23	20	14.9	30
7	5.0	15	17	20	13.8	30
8	5.0	15	20	20	11.8	28
9	5.0	15	23	20	9.8	27
10	7.5	5.0	17	25	28.1	35
11	7.5	5.0	20	25	27.5	35
12	7.5	5.0	23	25	26.8	35
13	7.5	10	17	25	24.3	34
14	7.5	10	20	25	22.9	33
15	7.5	10	23	25	21.6	33
16	7.5	15	17	25	20.5	32
17	7.5	15	20	25	18.4	31
18	7.5	15	23	25	16.3	30
19	10	5.0	17	30	34.7	36
20	10	5.0	20	30	34.7	36
21	10	5.0	23	30	33.4	36
22	10	10	17	30	30.9	35
23	10	10	20	30	29.5	35
24	10	10	23	30	28.1	34
25	10	15	17	30	27.0	34
26	10	15	20	30	24.9	33
27	10	15	23	30	24.3	32
28	5.0	0.0	0.0	20	24.3	38

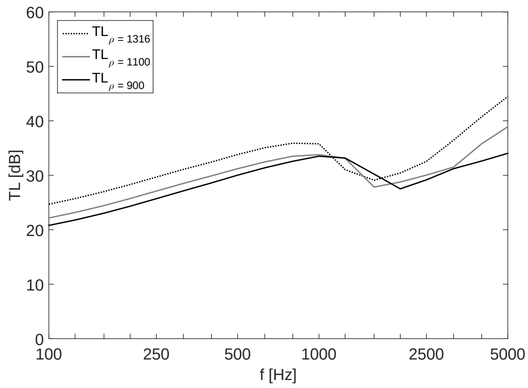

Figure 9: TL of a WPC sandwich plate, numerically computed using FTMM, assuming different material's densities.

mass approximately 70% larger than the original board. Even though configuration 28 provides the best acoustic performance, both in terms of TL and as single-number indicator R_w, given in Table 3, it should be noted that such a plate, made out of homogeneous solid beams, does not have many of the advantages provided by a sandwich element, being heavier and more expensive to be produced.

In order to devise a simple method to design WPC sandwich elements providing good acoustic performance it is necessary to understand how mass and flexural stiffness, related to the geometry of the cross-section, affect the TL of the orthotropic plate. Below the critical frequency, sound insulation is governed by the surface mass of the element μ. In Figure 12 the single-number sound insulation index R_w of all the 27 sandwich configurations is plotted against $10 \log \mu$. These data are correlated to a regression line based on the diffuse sound field mass-law [45], computed for the third octave band centred on 500 Hz, since the index R_w is weighted mostly around this

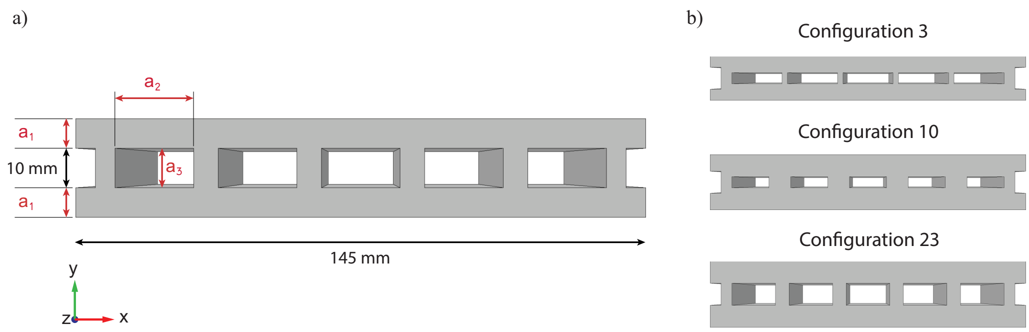

Figure 10: FEM-based parametric analysis on the x-beam's cross-section Three parameters are varied: a_1, a_2 and a_3, for a total of 27 configuration. The cross-sections obtained for configurations 3, 10, 23 are shown as example.

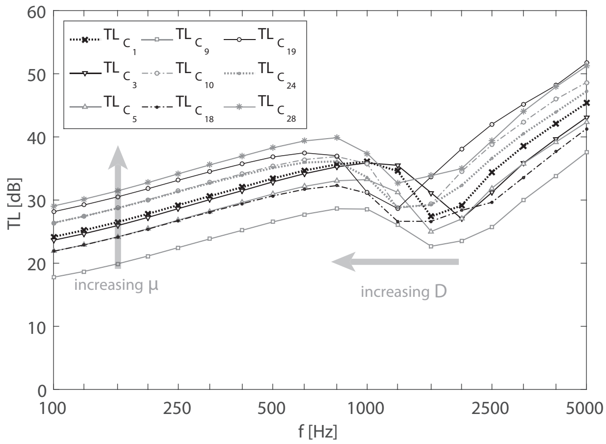

Figure 11: Some examples of the transmission loss of WPC plates obtained by bounding boards with optimised cross-section. Results simulated with FTMM.

frequency band.

It is not straightforward to find a correlation between the TL of the WPC panel and the beams' cross-section geometry in the region at and above the critical condition, which is controlled by its bending stiffness. Even though it is possible to predict the apparent bending stiffness of a sandwich beam for the frequency that tends to zero and to ∞, the rate of its decay is independent from these values and it has a significant influence on the frequency band the coincidence falls within. Moreover, due to the soft-orthotropy of the investigated panel, the bending stiffness is also dependent upon the azimuthal angle and the dip in the TL curves involves a wide frequency region that goes from the first coincidence to the critical condition. The fully numerical procedure, described in the previous section, represents a simple way to investigate the dynamic behaviour of an orthotropic sandwich plate during the optimisation process, although a simplified empirical formulation that correlates the material elastic properties and the structure's geometry to the decay rate of the frequency-dependent bending stiffness might be a handy tool for the design of sandwich plates. As discussed in paragraph 2.3 it is possible to identify a peculiar behaviour of the bending stiffness both in the low and in the high frequency ranges:

$$\begin{cases} D(f) \xrightarrow[f\to 0]{} D_s \\ \\ D(f) \xrightarrow[f\to\infty]{} D_l \end{cases} \tag{22}$$

Given that, by knowing the apparent bending stiffness of the 27 sandwich configurations, numerically determined along two directions, it was possible, from Eq. (7) and Eq. (6), to determine the constant Young's E_c and shear moduli G_c of the core, depending on coefficients A and B:

$$A = \frac{G_c h_c}{2\pi D_s \sqrt{\mu}}; \qquad B = \frac{G_c h_c}{2\pi \sqrt{\mu}} \tag{23}$$

A decreasing function, which respects the limit conditions expressed in Eq. (22), is assumed to be:

$$D_i(f) = (D_s - D_l)\,\mathrm{e}^{-\gamma f} + D_l \tag{24}$$

Published article available online: https://doi.org/10.1016/j.conbuildmat.2018.04.155

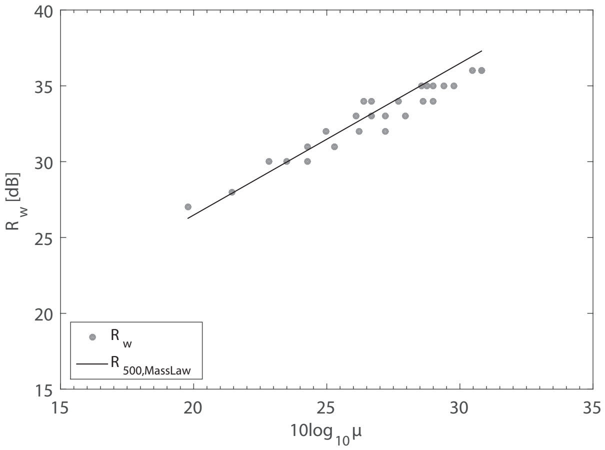

Figure 12: Correlation between the sound insulation index R_w and the surface mass of 27 optimised configurations of WPC boards.

The term γ has been determined from the 54 bending stiffnesses associated with the orthotropic directions of the parametric configurations. As shown in Figure 13, a good correlation has been found with the exponent γ and the term $B_i/\sqrt{\mu_i}$, where μ_i is the surface mass of the beam associated with the principal i-direction and B_i is the coefficient given in Eq. (23). Thus, by reformulating Eq. (24), it is possible to provide an empirical formulation in order to approximate the apparent bending stiffness decay rate with the frequency, which is a function of the material's static elastic constants and the surface mass of the structure:

$$D_i(\omega) = (D_s - D_l)\exp\left(\frac{19.881\omega\mu}{G_c h_c}\right) + D_l \tag{25}$$

The accuracy of such an empirical formulation has been investigated by comparing the critical frequencies along the x-direction, evaluated from the approximated bending stiffness given in Eq. (25), according to the dispersion relation in Eq. (11), to the critical frequencies determined from the wavenumbers obtained by means of the SFFT approach. Figure 14 shows the critical frequencies of all 27 sandwich configurations.

5. Conclusion

In this paper the sound insulation of an orthotropic panel, constituted by several WPC extruded boards bonded together, has been investigated. The WPC plate was modelled within a FTMM model as a thin orthotropic layer in order to compute the sound transmission loss. It was described by using frequency dependent stiffness properties, in order to take into account the complex dynamics of these structures by using a low-order theory. The apparent stiffness properties of a WPC board have been determined by means of a resonant numerical approach, based on an FE simulation. The method has been proved to be reliable by comparing the flexural stiffness, obtained from the FE analysis, with the experimental values measured on a WPC board by means of a resonant technique. The resonant methods, whether applied numerically or experimentally,

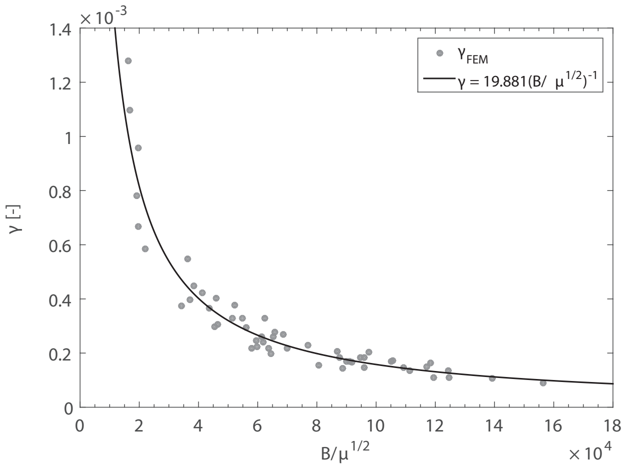

Figure 13: Correlation to determine the empirical formulation to approximate the apparent frequency-dependent bending stiffness of the plate.

are generally limited in frequency; in fact, it is not always possible to determine the resonances associated with the bending motion up to higher frequencies. An alternative approach based on spatial Fourier transform has been tested, finding consistent results. A numerically-based procedure to investigate the plate dynamics is particularly convenient for this kind of structures, since it allows the evaluation of the flexural stiffness along both principal orthotropic directions, which would otherwise be impossible experimentally. The orthotropic flexural stiffness in any given propagation direction, necessary as input data in the FTMM model, has been approximated with an elliptic interpolation of the stiffness determined along the two principal directions. Although this is an approximated approached, based on the assumption that the in-plane shear modulus is proportional to a combination of the elastic moduli along the principal directions, a remarkable agreement has been found between the transmission loss computed with the FTMM and the experimental curve. The WPC elements exhibit a soft-orthotropic behaviour: the difference between the stiffness associated with the principal directions is small and the two characteristic coincidences fall within neighbouring third-octave bands.

One of the most interesting applications of this fully numerical vibro-acoustic analysis is the optimization process to increase the acoustic performance of the structure. A parametric analysis, investigating the TL of 28 different geometric configurations of the WPC extruded boards, has been presented, varying their cross-section and consequently their surface mass and stiffness. A good correlation has been found between the mass-law for a diffuse sound field, computed at 500 Hz and the sound insulation index determined from the FTMM for all the 28 configurations. For sandwich elements the apparent bending stiffness decays as the frequency increases. The rate of the decay of the bending stiffness, associated with both principal directions, can be determined from the FEM structural dynamics models. Alternatively, an approximate empirical equation to evaluate the dynamic bending stiffness of a sandwich beam from the material's static elastic properties and the structure's geometric characteristics has been proposed. The results approximate with good accuracy the frequency-dependent bending stiffness, obtained from the FEM models, for all 27 sandwich configurations.

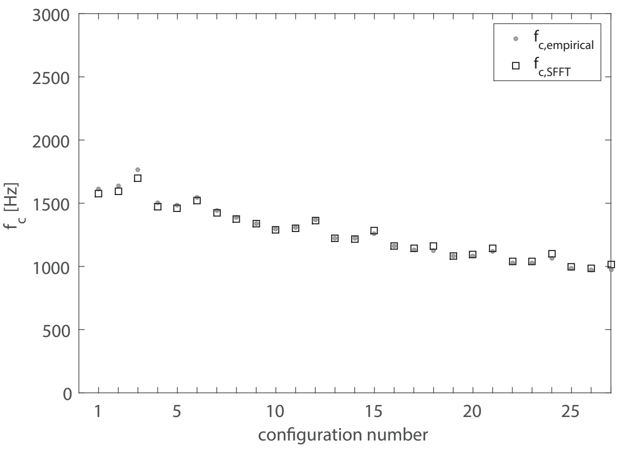

Figure 14: The critical frequencies along the *x*-direction computed from the wavenumbers, evaluated by using the SFFT approach, are compared to the values obtained from the empirical formulation for the apparent bending stiffness.

Acknowledgement

The authors would like to thank Maurizio Tarello and Massimiliano Tiengo of Adler Evo Villastellone, Turin (Italy), for providing the Oberst testing equipment. The authors are also deeply grateful to Andrea Pizzardi of the company Iperwood for providing the WPC boards.

References

[1] O. Adekomaya, T. Jamiru, R. Sadiku, Z. Huan, A review on the sustainability of natural fiber in matrix reinforcement–a practical perspective, Journal of Reinforced Plastics and Composites 35 (1) (2016) 3–7.
[2] E. Zini, M. Scandola, Green composites: an overview, Polymer composites 32 (12) (2011) 1905–1915.
[3] J. G. Gwon, S. Y. Lee, S. J. Chun, G. H. Doh, J. H. Kim, Physical and mechanical properties of wood–plastic composites hybridized with inorganic fillers, Journal of Composite Materials 46 (3) (2012) 301–309.
[4] J. Z. Lu, Q. Wu, I. I. Negulescu, Wood-fiber/high-density-polyethylene composites: Coupling agent performance, Applied polymer science 96 (1) (2005) 93–102.
[5] A. Schirp, J. Stender, Properties of extruded wood-plastic composites based on refiner wood fibres (tmp fibres) and hemp fibres, European Journal of Wood and Wood Products 68 (2) (2010) 219–231.
[6] K. Englund, V. Villechevrolle, Flexure and water sorption properties of wood thermoplastic composites made with polymer blends, Applied polymer science 120 (2) (2011) 1034–1039.
[7] V. Mazzanti, F. Mollica, N. El Kissi, Rheological and mechanical characterization of polypropylene-basedwood plastic composites, Polymer Composites 37 (12) (2016) 3460–3473.
[8] V. Mazzanti, F. Mollica, In-line rheometry of polypropylene based wood polymer composites, Polymer testing 47 (1) (2015) 30–35.
[9] H. Choe, G. Sung, J. H. Kim, Chemical treatment of wood fibers to enhance the sound absorption coefficient of flexible polyurethane composite foams, Composites Science and Technology.
[10] U. Berardi, G. Iannace, Acoustic characterization of natural fibers for sound absorption applications, Building and Environment 94 (2015) 840–852.
[11] F. Asdrubali, S. Schiavoni, K. Horoshenkov, A review of sustainable materials for acoustic applications, Building Acoustics 19 (4) (2012) 283–311.
[12] J. Zhao, X. M. Wang, J. Chang, Y. Yao, Q. Cui, Sound insulation property of wood–waste tire rubber composite, Composites Science and Technology 70 (14) (2010) 2033–2038.
[13] M. Munjal, Response of a multi-layered infinite plate to an oblique plane wave by means of transfer matrices, Journal of Sound and Vibration 162 (2) (1993) 333–343.

[14] E. Nilsson, A. Nilsson, Prediction and measurement of some dynamic properties of sandwich structures with honeycomb and foam cores, Journal of sound and vibration 251 (3) (2002) 409–430.
[15] A. Santoni, S. Schoenwald, B. Van Damme, P. Fausti, Determination of the elastic and stiffness characteristics of cross-laminated timber plates from flexural wave velocity measurements, Journal of Sound and Vibration 400 (2017) 387–401.
[16] ASTM E756-05 – Standard Test Method for Measuring Vibration-Damping Properties of Materials, Standard, ASTM International, West Conshohocken, PA, USA (2010).
[17] J. L. Wojtowicki, L. Jaouen, R. Panneton, New approach for the measurement of damping properties of materials using the oberst beam, Review of scientific instruments 75 (8) (2004) 2569–2574.
[18] R. Pereira, J. P. Arenas, E. Zumelzu, Comparison of four test methods to measure damping properties of materials by using piezoelectric transducers, Materials & Design 32 (4) (2011) 2423–2428.
[19] A. C. Nilsson, Wave propagation in and sound transmission through sandwich plates, Journal of Sound and Vibration 138 (1) (1990) 73–94.
[20] S. Kumar, L. Feng, U. Orrenius, Predicting the sound transmission loss of honeycomb panels using the wave propagation approach, Acta Acustica united with Acustica 97 (5) (2011) 869–876.
[21] D. Backström, A. C. Nilsson, Modelling the vibration of sandwich beams using frequency-dependent parameters, Journal of Sound and Vibration 300 (3) (2007) 589–611.
[22] G. A. Papagiannopoulos, G. D. Hatzigeorgiou, On the use of the half-power bandwidth method to estimate damping in building structures, Soil Dynamics and Earthquake Engineering 31 (7) (2011) 1075–1079.
[23] B. Van Damme, A. Zemp, Measuring dispersion curves for bending waves in beams: A comparison of spatial fourier transform and inhomogeneous wave correlation, Acta Acustica united with Acustica 114 (2018) 228–234.
[24] N. B. Roozen, L. Labelle, Q. Leclere, K. Ege, S. Alvarado, Non-contact experimental assessment of apparent dynamic stiffness of constrained-layer damping sandwich plates in a broad frequency range using a nd: Yag pump laser and a laser doppler vibrometer, Journal of Sound and Vibration 395 (2017) 90–101.
[25] A. Nilsson, B. Liu, Vibro-acoustics, Vol. 1, Science Press, Beijing and Springer-Verlag, Berlin Heidelberg, 2015.
[26] E. Piana, P. Milani, N. Granzotto, Simple method to determine the transmission loss of gypsum panels, in: Proceedings of the 21nd International Congress on Sound and Vibration Proceedings, Vol. 21, International Institute of Acoustics and Vibration, Beijing, China, 2015.
[27] F. Leppington, K. Heron, S. M. Mead, Resonant and non-resonant acoustic properties of elastic panels. I. The radiation problem, Proc. R. Soc. Lond. A 406 (1831) (1986) 139–171.
[28] A. Santoni, P. Bonfiglio, P. Fausti, S. Schoenwald, Predicting sound radiation efficiency and sound transmission loss of orthotropic cross-laminated timber panels, in: Proceedings of Meetings on Acoustics 173EAA, Vol. 30, ASA, 2017, p. 015013.
[29] A. Santoni, P. Bonfiglio, P. Fausti, S. Schoenwald, H. M. Tröbs, Sound radiation efficiency measurements on cross laminated timber plates, in: Proceedings of the 45th International Congress and Exposition on Noise Control Engineering, Institute of Noise Control Engineering, Hamburg, Germany, 2016, pp. 3697–3707.
[30] J. L. Guyader, C. Lesueur, Acoustic transmission through orthotropic multilayered plates. Part II: transmission loss, Journal of Sound and Vibration 58 (1) (1978) 69–86.
[31] J. L. Guyader, C. Lesueur, Transmission of reverberant sound through orthotropic, viscoelastic multilayered plates, Journal of Sound and Vibration 70 (3) (1980) 319–332.
[32] R. R. Wareing, J. L. Davy, J. R. Pearse, The sound insulation of single leaf finite size rectangular plywood panels with orthotropic frequency dependent bending stiffness, The Journal of the Acoustical Society of America 139 (1) (2016) 520–528.
[33] H. J. Lin, C. N. Wang, Y. M. Kuo, Sound transmission loss across specially orthotropic laminates, Applied Acoustics 68 (10) (2007) 1177–1191.
[34] Y. M. Kuo, H. J. Lin, C. N. Wang, Sound transmission across orthotropic laminates with a 3d model, Applied Acoustics 69 (11) (2008) 951–959.
[35] N. Atalla, Modeling the sound transmission through complex structures with attached noise control materials, Wave Motion 51 (4) (2014) 650–663.
[36] D. Rhazi, N. Atalla, Transfer matrix modeling of the vibroacoustic response of multi-materials structures under mechanical excitation, Journal of sound and vibration 329 (13) (2010) 2532–2546.
[37] P. Bonfiglio, F. Pompoli, K. V. Horoshenkov, M. I. B. S. A. Rahim, A simplified transfer matrix approach for the determination of the complex modulus of viscoelastic materials, Polymer Testing 53 (2016) 180–187.
[38] A. Santoni, P. Bonfiglio, J. L. Davy, P. Fausti, F. Pompoli, L. Pagnoncelli, Sound transmission loss of ETICS cladding systems considering the structure-borne transmission via the mechanical fixings: Numerical prediction model and experimental evaluation, Applied acoustics 122 (2017) 88–97.
[39] J. Allard, N. Atalla, Propagation of sound in porous media: modelling sound absorbing materials, 2nd Edition, John Wiley & Sons, Ltd, Chichester, UK, 2009.
[40] M. Villot, C. Guigou-Carter, L. Gagliardini, Predicting the acoustical radiation of finite size multi-layered structures

by applying spatial windowing on infinite structures, Journal of sound and vibration 245 (3) (2001) 433–455.

[41] D. Rhazi, N. Atalla, A simple method to account for size effects in the transfer matrix method, The Journal of the Acoustical Society of America 127 (2) (2010) EL30–EL36.

[42] P. Bonfiglio, F. Pompoli, R. Lionti, A reduced-order integral formulation to account for the finite size effect of isotropic square panels using the transfer matrix method, The Journal of the Acoustical Society of America 139 (4) (2016) 1773–1783.

[43] T. E. Vigran, Predicting the sound reduction index of finite size specimen by a simplified spatial windowing technique, Journal of Sound and Vibration 325 (3) (2009) 507–512.

[44] ISO 15186-1 – Acoustics – Measurement of sound insulation in buildings and of building elements using sound intensity – Part 3: Laboratory measurements., Standard, International Organization for Standardization, Geneva, CH (2003).

[45] T. E. Vigran, Building acoustics, Taylor & Francis, New York, NY, USA, 2008.